



# Columnar aggregates of crown ether substituted phthalocyanines perpendicularly anchored on a surface via a selective binding site

Thierry Thami, Christophe Chassenieux, Christian Frétigny, Jean-Paul Roger, Felix Steybe

## ► To cite this version:

Thierry Thami, Christophe Chassenieux, Christian Frétigny, Jean-Paul Roger, Felix Steybe. Columnar aggregates of crown ether substituted phthalocyanines perpendicularly anchored on a surface via a selective binding site. *Journal of Porphyrins and Phthalocyanines*, 2002, 6 (9), pp.563 - 570. 10.1142/S1088424602000701 . hal-01726386

**HAL Id: hal-01726386**

**<https://hal.umontpellier.fr/hal-01726386>**

Submitted on 27 Jan 2021

**HAL** is a multi-disciplinary open access archive for the deposit and dissemination of scientific research documents, whether they are published or not. The documents may come from teaching and research institutions in France or abroad, or from public or private research centers.

L'archive ouverte pluridisciplinaire **HAL**, est destinée au dépôt et à la diffusion de documents scientifiques de niveau recherche, publiés ou non, émanant des établissements d'enseignement et de recherche français ou étrangers, des laboratoires publics ou privés.

**Columnar Aggregates of Crown Ether Substituted Phthalocyanines  
Perpendicularly Anchored on a Surface via a Selective Binding Site**

Thierry Thami<sup>1, 2</sup> \*, Christophe Chassenieux<sup>2</sup>, Christian Fretigny<sup>2</sup>, Jean-Paul Roger<sup>3</sup>,  
and Felix Steybe<sup>1</sup>

<sup>1</sup> Laboratoire de Chimie Inorganique et Matériaux Moléculaires, CNRS ESA 7071,  
ESPCI 10, rue Vauquelin F-75231 Paris cedex 05, France

<sup>2</sup> Laboratoire de Physico-chimie des Polymères et des Milieux Dispersés, CNRS UMR  
7615, ESPCI 10, rue Vauquelin F-75231 Paris cedex 05, France

<sup>3</sup> Laboratoire de Spectroscopie en Lumière Polarisée, CNRS UPR A0005, ESPCI 10,  
rue Vauquelin F-75231 Paris cedex 05, France

\* Corresponding author : Thierry Thami, Institut Européen des Membranes, UMR CNRS 5635, UMII-  
CC047, Place Eugène Bataillon, 34095 Montpellier cedex 5, France

*E-mail address:* thierry.thami@iemm.univ-montp2.fr

**ABSTRACT:** The purpose of this work is to anchor perpendicularly to a surface the aggregates obtained by complexation of crown-ether substituted lutetium bisphthalocyanine, [(15C5)<sub>4</sub>Pc]<sub>2</sub>Lu, in the presence of KSCN. In order to orientate these aggregates perpendicularly to the substrate, silica surface is grafted with an unsymmetrical lutetium bisphthalocyanine substituted, on one macrocycle by four crown ether subunits, and on the other one with four lateral chains terminated by a carboxylic group. The latter compound is used as a *selective binding site* to anchor pillar-like aggregates formed in solution. The aggregates were characterized in mixture of chloroformic solution by UV-visible and light scattering experiments. This permits to evidence the formation of rod-like particles in the presence of an excess of KSCN. Then, the aggregates were deposited on surfaces and their morphologies were studied by atomic force microscopy (AFM). In the case of substrates having non-specific binding sites such as silica and functionalized silica with 3-trimethoxypropylaminosilane, rods were observed lying parallel on the surfaces. In the case of the substrate grafted with the selective binding site, single columns of these supramolecular assemblies perpendicularly to the surface have been observed by AFM.

**KEYWORDS:** Lutetium bisphthalocyanine; crown-ether; aggregation; grafted surface; AFM

## INTRODUCTION

Aggregation in solution of substituted or unsubstituted metallophthalocyanine is known from earlier studies (see references mentioned in [1]). It has been shown that in the absence of any cation, polar solvents induce the formation of aggregates of poorly defined geometry.

With crown-ether substituted monophthalocyanine in the presence of small cations such as  $\text{Na}^+$  which can be incorporated within the crown ether cavity, no drastic change of the UV-visible absorption spectra is generally observed. Aggregation probably does not occur. The nature of the anion however can sometimes promote the aggregation. For example sodium acetate yields aggregates in  $\text{CHCl}_3$  whereas  $\text{NaSCN}$  does not [2]. In the presence of larger cations forming sandwich complexes only cofacial dimer [2,3] can be formed. Electron Spin Resonance and Magnetic Circular Dichroism studies have been carried out to characterize the dimerization processes of crown ether substituted lutetium bisphthalocyanines as a function of the solvent composition [4,5].

Crown-ether substituted phthalocyanines have been described since 1986 [6-8]. The corresponding lutetium bisphthalocyanine,  $[(15\text{C}5)_4\text{Pc}]_2\text{Lu}$  (molecule **1** in Fig. 1a), was synthesized three years later [9]. Previous studies of cation induced aggregation of this compound were carried out in solution. With cations such as potassium or rubidium ions, this compound has been shown to yield pillar-like high molar mass aggregates by forming sandwich like complexes [10-12]. The complexation processes and the formation of aggregates have both been shown to be governed by positive cooperative effects. The supramolecular aggregates obtained via cooperative complexation of  $[(15\text{C}5)_4\text{Pc}]_2\text{Lu}$  in the presence of  $\text{KSCN}$  salt is shown in Figure 1b. This process

yields pillar-like structure in solution which is ion-induced by sandwich-stacking of the monomeric units and  $K^+$  (stoichiometry of one ligand **1** for four  $K^+$ ).

**Fig. 1a      Fig. 1b**

The cooperativity is provided by the molecular characteristics of the ionophore with a central rigid core symmetrically substituted by four ionophore subunits. The process of complexation of the ionophore subunits involves four steps defined by the constants of complexation  $K_1$ ,  $K_2$ ,  $K_3$ ,  $K_4$ . To explain the formation of high molar mass columnar aggregate, it must be postulated that  $K_4 \gg K_1, K_2, K_3$  [12]. The experimental challenge is then to anchor single column of aggregate perpendicularly to a surface in order to yield, in a further step, two-dimensional systems. We show here that this can be achieved by judiciously grafting a substrate creating a selective binding site (Fig. 2): the bisphthalocyanine derivative **2** realizes the connection between the surface and the column.

**Fig. 2**

In a first step, we have synthesized [13] an unsymmetrical lutetium bisphthalocyanine substituted, on one macrocycle by four crown ether subunits, and on the other one with four lateral chains terminated by a carboxylic group (molecule **2** in Fig. 2). Then **2** is covalently coupled on an aminosilane functionalized silica surface in order to favor a crown-ether substituted macrocycle orientation parallel to the surface as shown in Fig. 2. This paper describes the characterization in solution of the aggregates of  $[(15C5)_4Pc]_2Lu$  by UV-visible absorption spectra and light scattering and, in a second step, the observation by Atomic Force Microscopy (AFM) of the supramolecular aggregates on silica surfaces either functionalized or grafted.

## EXPERIMENTAL

### Solvents

To improve the reproducibility of the aggregate formation in solution and their deposition on silica surfaces, a solvent mixture  $\text{CHCl}_3/\text{MeOH}/\text{H}_2\text{O}$  has been chosen. In such a solvent, the state of hydration of silica surfaces is well defined [14,15]. Moreover, in this solvent, the solvation shell of ionic species is controlled. The volumic fraction of  $\text{CHCl}_3$  over  $\text{MeOH}/\text{H}_2\text{O}$  ranged from 98 to 95% while the volumic fraction of  $\text{MeOH}/\text{H}_2\text{O}$  was kept constant and equal to 95/5% by volume. The solvents mixtures were prepared from chloroform (SDS) filtrated on aluminium oxide, from methanol (SDS) distilled on  $\text{CaH}_2$  and from ultrapure water. S98 = 98/1.9/0.1% and S95 = 95/4.75/0.25.% by volume.

### Absorption spectroscopy

Electronic spectra were recorded on a Kontron Uvikon 860 spectrophotometer. All measurements were performed in 1 cm quartz cells. Aggregation studies were carried out by recording the changes of the absorption spectra at 667 nm resulting from addition of KSCN ( $10^{-2}$  M) to 2 ml of S98 solution ( $10^{-5}$  M) of **1**. The KSCN salt (Aldrich) was dissolved under ultrasonic stirring in the S90 mixture (S90 = 90/9.5/0.5% v/v) and was added portionwise with a microsyringe.

### Static light scattering

Static light scattering measurements were carried out with an experimental set-up described in reference [16]. The wavelength used was 514 nm to minimize absorption problems due to the lutetium derivative. A correction of the absorption of scattered light has been derived from the corresponding UV-visible spectra. The solution of **1** ( $10^{-5}$  M in S98) and KSCN ( $10^{-2}$  M in S90) were filtered through 0.5  $\mu\text{m}$

Millipore filters into cells (diameter of 12 mm). The potassium salt in S90 was added to 2 ml of **1** in S98. The scattered intensity in the  $\theta$  direction was measured for different ratio  $r = [\text{K}^+]/[\text{1}]$  ranging from  $r = 0$  to  $r = 32$ . Toluene was used as a reference for the Rayleigh ratio  $R_\theta$ . The angular range  $\theta$  of the goniometer was 20-140°. The weight-averaged apparent molar mass  $M_w$  were determined by extrapolating to  $\theta = 0$  the  $Kc/R_\theta$  versus  $q^2$  curves where  $c$  is the concentration of the aggregate derived from UV-visible absorption measurements,  $q$  is the wave vector,  $R_\theta$  is the measured Rayleigh ratio and  $K$  is a constant defined as:

$$K = \frac{4\pi^2}{N\lambda^4} n^2 \left( \frac{dn}{dc} \right)^2$$

where  $n$  is the refractive index of toluene,  $\lambda$  is the wavelength of the laser light,  $N$  is the Avogadro's number and  $dn/dc$  is the refractive index increment. Refractive index measurements were performed at different values of the ratio  $r$  with a differential refractometer R404 (white light) (Water Associates) at 25°C.

### **Spectroscopic ellipsometry [17-19]**

A SOPRA ES 4G spectroscopic ellipsometer was used. The optical system was constituted by a rotating polarizer and an analyzer. The diameter of the focussed beam spot was 150  $\mu\text{m}$ . The angle of incidence on the sample was 75°. All samples were derived from silicon (100) wafers. The ellipsometric parameters  $\cos\Delta$  and  $\tan\Psi$  were recorded as a function of the wavelength ( $\Delta$  is the phase difference and  $\tan\Psi$  is the amplitude ratio of the complex reflexion coefficients of the electrical field components parallel and perpendicular to the plane of incidence). The film thickness and the refractive index calculations were carried out from ellipsometric parameters using

standard models for optically isotropic media [18]. The optical anisotropy possibly induced by functionalization of the silica surface either with the 3-aminopropyl trimethoxysilane or with the carboxylic acid-functionalized bisphthalocyanine **2** has not been taken into account in the thickness calculation. This should lead to a minor under or overestimation of the film thickness [20].

The thickness of the functionalized layer ( $\text{SiO}_2$  natural oxidation of silicon treated with the trimethoxysilane derivative) was determined by comparison with a bare substrate (thickness about 2 nm). Thickness values were obtained by using six different wavelengths in the range 0.45-0.5  $\mu\text{m}$ . We assumed in the case of the amino-functionalized substrate that the refractive index of the  $\text{SiO}_2$  functionalized layer was equivalent to that of ungrafted silica ( $n = 1.46$ ).

The thickness of the grafted layer with **2** was determined from the ellipsometric parameters recorded in the UV-visible region from 0.26 to 0.85  $\mu\text{m}$  (237 points). In this calculation a bilayer structure was postulated. The first layer is made up of the trimethoxysilane derivative reacted with the silica surface and the  $\text{SiO}_2$  underneath. The second layer is constituted of the grafted lutetium bisphthalocyanine. The values of the real and the imaginary parts of the refractive index,  $n-ik$ , were measured independently on oxidized thin film of **1** since the compounds **1** and **2** readily oxidize in the presence of air.

Thin films of **1** were prepared by spin-coating of **1** in  $\text{CHCl}_3$  deposited onto a silicon wafer. The coated layer was then exposed to bromine vapor for 5 min and left in air 1 hour before the measurements. The relative intensities of the absorption bands as well as the maximum wavelengths of  $1^+,\text{Br}^-$  determined by UV-visible absorption spectra (506 nm; 707 nm; 997 nm) on thin films (thickness 65 nm) deposited on glass



slides, are in good agreement with ellipsometric results. An independent measurement of the thickness was carried out by AFM-imaging a zone where scratches have been performed by the tip. Both results are in a very satisfactory agreement confirming our calibration method.

In addition, glass substrate is used to check the optical absorption spectra and the thickness of the lutetium bisphthalocyanine derivative **2** layer. The thickness of the layer was calculated from the Beer-Lambert law:

$$A = \varepsilon \frac{d}{M} e$$

where  $A$  is the absorbance of the layer,  $d$  the density,  $M$  the molar mass,  $\varepsilon$  the extinction coefficient and  $e$  the thickness of the layer. The value of the density and the extinction coefficient of the layer is deduced from the  $k$ -value determined by ellipsometry:

$$\varepsilon \frac{d}{M} = \frac{4\pi k}{\lambda} \frac{1}{\ln 10}$$

where  $\lambda$  is the wavelength considered.

### **Atomic force microscopy (AFM)**

Tapping mode AFM has been used to image the samples (Digital Instrument Nanoscope IIIa). AFM provides informations on surface structures at a molecular scale. For reviews associated to chemistry related problems see references [21,22]. The sensor was a silicon crystal cantilever with a spring constant of 20-80 N/m and a resonant frequency of about 300 kHz. For standard sensors, the typical tip radius is 10 nm. For higher resolution studies a Supersharpsilicon sensor (Nanosensors) with nominal radius of 2 nm was used. The roughness of the sample was extracted from the half width of the histogram ( $256 \times 256$  pixels for  $1 \mu\text{m}^2$ ).

### **Preparation and characterization of the samples**

The grafted substrate with **2** has been prepared in two steps (i) functionalization of a properly activated silica surface, (ii) grafting of the molecular derivative **2** used, in a further step, as an anchoring site for the columnar aggregates (see Fig. 2).

The silica surface of the wafer (Siltronix) was cleaned with a mixture  $\text{H}_2\text{SO}_4/\text{H}_2\text{O}_2$  (70:30; v/v) at  $90^\circ\text{C}$ , rinsed with ultrapure water, dried in a stream of nitrogen and heated at  $110^\circ\text{C}$  for 20 min. Under these conditions, approximately  $5 \times 10^{14}$  silanol groups per  $\text{cm}^2$  are obtained [23] and the silica surface remains hydrated [20,24-25]. 3-aminopropyl trimethoxysilane (Aldrich) in toluene (0.5%; v/v) was reacted with the  $\text{SiO}_2$  surface at  $110^\circ\text{C}$ . After rinsing (toluene;  $\text{CHCl}_3/\text{MeOH}$ , 2:1, v/v), the sample was dried ( $\text{N}_2$ ) and cured at  $110^\circ\text{C}$  (20 min). The thickness of the aminosilane functionalized silica surface is  $3.3 \pm 0.2$  nm from ellipsometric measurements which corresponds to about four monolayers (0.7 nm) at least of aminosilane.

Grafting of **2** is performed on aminosilane functionalized silica surface of silicon wafers and on glass slides used as references. The substrates were dipped into a solution of **2** ( $5 \times 10^{-4}$  M in  $\text{CHCl}_3/\text{MeOH}$ , 95/5% v/v). Ammonium salts between the four carboxylic groups of **2** and the amino-groups linked to the surface probably form at that stage. The dip coated substrates were then immersed into a solution ( $5 \times 10^{-3}$  M) of dicyclohexylcarbodiimide (DCC) in toluene under reflux in order to achieve covalent linkage. On the reference glass slides, a tenfold decrease of the absorbance is noticed in approximately 10 min after which a stationary state is reached: only the covalently linked phthalocyanine derivatives are thought to remain on the surface. After rinsing ( $\text{CHCl}_3/\text{MeOH}$ , 2:1, v/v), the sample was dried ( $\text{N}_2$ ) and the reality of the grafting process was evidenced by spectroscopic ellipsometry and UV-visible absorption spectroscopy. In this case a thickness of  $2.1 \pm 0.2$  nm is derived from UV-visible

spectra (glass slide). Spectroscopic ellipsometry on **2** grafted on the aminosilane functionalized silica of the wafer yields a thickness of  $2.0 \pm 0.2$  nm for the same conditions of treatment.

Further informations about the spatial molecular arrangement have been gained from Atomic Force Microscopy. The half width of the histogram peak gives a roughness of about 0.7 nm for the aminosilane functionalized silica wafer. After grafting of **2**, a higher value of about 1.8 nm may be extracted. Thus in both case, the organic layers are rather flat at a molecular scale.

### **Deposition on the surfaces**

The substrates grafted with **2** are then immersed for 40 min into dilute solutions of **1**/KSCN ( $[1] = 10^{-5}$  M and  $[KSCN] = 1.6 \cdot 10^{-4}$  M in S95 corresponding to the ratio  $r = 16$ ). The samples are dried under a stream of nitrogen. For comparison, the same experiments were carried out on unmodified silica (SiO<sub>2</sub>) or functionalized silica with 3-aminopropyl trimethoxysilane.

## **RESULTS AND DISCUSSION**

The various aggregation processes have been studied by UV-visible absorption spectroscopy and light scattering in the CHCl<sub>3</sub>/MeOH/H<sub>2</sub>O (S98) solvent mixture. The UV-visible absorption spectra are used to follow the disappearance of the monomeric species [(15C5)<sub>4</sub>Pc]<sub>2</sub>Lu at 667 nm as a function of the cation to the lutetium derivative concentrations ratio ( $r = [K^+]/[1]$ ) when KSCN salt was added in the chloroform based mixture ( $[1] = 10^{-5}$  M in S98;  $[KSCN] = 10^{-2}$  M in S90). The spectroscopic changes as the concentration of KSCN increase are roughly the same as those previously reported [12]. When following the concentration of **1** versus  $r$ , a linear dependence is obtained

from  $r = 0$  to  $r \sim 4$  with a slope of about 4/1 and then a plateau value is observed from  $r \sim 4$  (Fig. 3). This is an indication that the complexation process in this solvent mixture yields (via positive cooperative effects [11]) one-dimensional aggregates as shown in Fig. 1b, since the ratio 4/1 can only be obtained for high molar mass pillar-like aggregates.

### Fig. 3

Light scattering measurements allow us to obtain further insight regarding the molecular properties of the aggregates in terms of size and molar mass. Moreover their “shape” can be estimated from the  $q$ -dependence of the scattered intensity in the high  $q$  range ( $q$  is the wave vector). All these results are summarized in Table 1.

### Table 1

For small  $r$  values, high molar mass aggregates are obtained, their distribution in sizes is highly polydisperse. Moreover, these aggregates are dense. When  $r$  increases above 8, the density, the molar mass and the polydispersity of the aggregates highly decrease. For the highest  $r$  value investigated ( $r = 32$ ),  $I$  scales as  $q^{-1}$ . This behaviour is expected for rod-like particles. For small  $r$  values, high molar mass and dense aggregates can coexist with rod-like species. A deaggregation process must take place leading to rod-like particles for high values of  $r$ . For this reason, the deposition on surfaces has been performed in the presence of an excess of KSCN. Moreover, these conditions probably favor the attachment of the columns on the selective binding sites since complexation of cations to these latter is a prerequisite.

The deposition of the aggregates has been first carried out on silica and on propylaminosilane functionalized surfaces. The figures 4a and 5a show the corresponding AFM images. In both cases rods are observed lying on the substrate

plane with maximum lengths of the order of 100 nm. The height profiles of the rods (Fig. 4b and 5b) give an estimation of the diameter of about 1.5-2 nm on silica and 3-5 nm on amino-functionalized silica. This is compatible with the theoretical diameter of the disk-shaped (15C5)<sub>4</sub>PcM molecule (2.8 nm) as determined by X-ray crystallography [26]. As a result of the convolution by the tip, the width of the rods is found to be larger (15-20 nm). In order to estimate the tip convolution effect, AFM images on DNA molecules deposited on mica have been made. Indeed, the diameter (2 nm) of the molecule is theoretically comparable to the one of the aggregates derived from **1**. A 1 nm height and 12 nm width are measured for DNA under the same imaging conditions. These two values are in accordance with the measurements made on the aggregates lying parallel to the two substrates studied.

**Fig. 4a      Fig. 4b      Fig. 5a      Fig. 5b**

AFM images have been obtained on the **2** grafted functionalized silica surface: the AFM images obtained after 40 min is shown in Figure 6a. Two different species can be readily identified: isolated spots which can be associated with columnar aggregates perpendicularly oriented to the surface together with small crystals lying on the surface. Indeed, it can be seen in Fig. 6a that many small crystals (gray), about 5-15 nm height are present on the surface. Isolated spot (white), about 15-25 nm height are also clearly visible. The diameters of the spot, ranging from 5 nm to 40 nm, are seen to depend on their heights (5 nm to 25 nm). Such a correlation is expected from the tip-convolution effect previously described and is compatible with the presence of pillar-like aggregates perpendicular to the substrate. Deformation of the columns due to mechanical interaction with the tip in tapping mode may eventually occur. However, for the presented experiments, no topographical change is observed by varying the

experimental conditions (at least when they are kept “soft”: low free amplitude and low amplitude reduction for imaging). Though the possibility that the tip knocks down the columns cannot be definitely ruled out, this situation seems rather improbable. It is worth stressing that all the columns identified seem perpendicular to the substrate. However, because polymers (3D-network) or multilayers of aminosilane are created (see experimental section), the carboxylic acid grafted bisphthalocyanine could be connected to amine groups in different layers and could induce a tilt of the columnar aggregates but, deviation from a 90° angle would probably lead to a strong tendency for the columns to collapse.

The grafted molecule **2** acts as a specific binding site by forming sandwich complexes in the presence of  $K^+$ . The binding of the aggregate on the anchoring molecule is very probably enhanced by the nonlinear nature of the complexation associated with the four ionophore subunits. In the presented experiments, the in-solution grown aggregates are reacted with the surface bound crown-ether substituted bisphthalocyanine molecules. Instead, the columns may directly grow from the surface. In situ characterization, nucleation and growth of the columnar aggregates, should be further studied. Attempts have also been made to use a sharper AFM tip (nominal radius of the tip: 2 nm) in order to see molecular details within the columns (Fig. 7). Further work is in progress in order to improve the quality of the AFM by eliminating humidity or adhesion effects.

**Fig. 6a      Fig. 6b      Fig. 7**

## CONCLUSION

The AFM observations on silica or amino-functionalized silica surfaces having non specific binding site demonstrate the rod-like nature of the aggregates. The shape of the aggregates determined by AFM is well correlated with light scattering measurement. In the case of the substrate grafted with molecule **2**, a different arrangement is observed by comparison with the previous substrates. The observation of single spots having height of 15-25 nm, reveals the presence of columnar aggregates perpendicularly oriented to the surface. In spite of the enlarging effect of the AFM tip, we have shown that it is possible to identify *individual* pillar-like aggregates by using a properly designed molecule to anchor them perpendicularly to the surface. Unsubstituted lutetium bisphthalocyanine has been shown to be the first intrinsic molecular semiconductor [29]. Moreover, the  $\text{Pc}_2\text{Lu}$  core of the columns could have interesting electrochemical, optical, electrical and magnetical properties [30,31]. The columnar aggregates thus formed are therefore constituted of electrically active units which can be used as an electrical nanowire. Moreover, the use of positive cooperative complexation processes to form the aggregates and their selective binding on the surface opens the field of Ionoelectronics [11,12,30]. Work is in progress in these two directions.

## Acknowledgments

The authors thank Prof. J. Simon for his collaboration and his useful comments on the manuscript. Many students, mainly from ESPCI, made part of the work presented in this publication. An exhaustive list is almost impossible to give but J. Agin, S.

Colette, V. Marchi and C. Vautrin are particularly acknowledged. T. Toupance and C. Teillet are both acknowledged for the synthesis of compound **1**. P. Bassoul is thanked for the drawing from X-ray data. This research was financially supported by EC grant 940558, by ESPCI and by the CNRS.

## REFERENCES AND NOTES

- [1] Pernin D, Simon J. *Mol. Cryst. Liq. Cryst. Sci. Technol., Sect. A* 2001; **355**: 457.
- [2] Sielken OE, van Tilborg MM, Roks MFM, Hendriks R, Drenth W, Nolte RJM. *J. Am. Chem. Soc.* 1987; **109**: 4261.
- [3] Kobayashi N, Lever ABP. *J. Am. Chem. Soc.* 1987; **109**: 7433.
- [4] Ishikawa N, Kaizu Y. *Chem. Phys. Lett.* 1993; **203**: 472.
- [5] Ishikawa N, Kaizu Y. *Chem. Lett.* 1998; 183; Ishikawa N, Kaizu Y. *J. Phys. Chem. A* 2000; **104**: 10009.
- [6] Koray AR, Ahsen V, Bekâroğ lu Ö. *J. Chem. Soc., Chem. Commun.* 1986; 932.
- [7] Hendriks R, Sielcken OE, Drenth W, Nolte RJM. *J. Chem. Soc., Chem. Commun.* 1986; 1464.
- [8] Kobayashi N, Nishiyama Y. *J. Chem. Soc., Chem. Commun.* 1986; 1462.
- [9] Bardin M, Bertounesque E, Plichon V, Simon J, Ahsen V, Bekâroğ lu Ö. *J. Electroanal. Chem.* 1989; **271**: 173.
- [10] Toupance T, Ahsen V, Simon J. *J. Chem. Soc., Chem. Commun.* 1994; 75.
- [11] Toupance T, Ahsen V, Simon J. *J. Am. Chem. Soc.* 1994; **116**: 5352.
- [12] Toupance T, Benoit H, Sarazin D, Simon J. *J. Am. Chem. Soc.* 1997; **119**: 9191.
- [13] Steybe F, Simon J, *New J. Chem* 1998; **22**: 1305.



- [14] Bauer D personal communication. A detailed treatment can be found in ref. [15].
- [15] Rosset R, Caude M, Jardy A. *Chromatographies en phases liquide et supercritique*, Masson: Paris, 1991; 237.
- [16] Chassenieux C, Johannsson R, Durand D, Nicolai T, Vanhoorne P, Jérôme R. *Colloids and Surfaces A: Physicochemical and Engineering Aspects* 1996; **112**: 155.
- [17] Aspnes DE, Theeten JB, Hottier F. *Phys. Rev.* 1979; **B20**: 3292.
- [18] Bernoux F, Piel JP, Lecat JH, Stehlé JL. *Techniques de l'Ingénieur Traité Mesures et Contrôle* R6 490-1, Techniques de l'Ingénieur: Schiltigheim, 1999.
- [19] Boccara AC, Pickering C, Rivory J.. Spectroscopic Ellipsometry, *Proc. of the 1st Int. Conf. on Spectroscopic Ellipsometry*, Elsevier: Amsterdam, 1993.
- [20] Parikh AN, Allara DL, Ben Azouz I, Rondelez F. *J. Phys. Chem.* 1994; **98**: 7577.
- [21] Frommer J. *Angew. Chem. Int. Ed. Engl.* 1992; **31**: 1298.
- [22] Takano H, Kenseth JR, Wong SS, O'Brien JC, Porter MD. *Chem. Rev.* 1999; **99**: 2845.
- [23] Perrot H, Jaffrezic N, Clechet P. *J. Electrochem. Soc.* 1990; **137**: 598.
- [24] Thiel PA, Madey E. *Surf. Sci. Rep.* 1987; **7**: 211. Mentioned in reference [25].
- [25] Silberzan P, Léger L, Ausserré D, Benattar JJ. *Langmuir* 1991; **7**: 1647.
- [26] From previous X-ray data of the uncomplexed crown-ether copper phthalocyanine [27] and  $\text{Pc}_2\text{Lu}$  [28] and from examination of molecular

models, the dimensions of **1** are about  $2.8 \times 2.8 \times 0.8 \text{ nm}^3$ . Thus, the diameter of the disk-shaped molecule is 2.8 nm.

- [27] Sirlin C, Bosio L, Simon J, Ahsen V, Yilmazer E, Bekâröğ lu Ö. *Chem. Phys. Lett.* 1987; **139**: 362.
- [28] Darovskikh AN, Tsytsenko AK, Frank-Kamenetskaya OV, Fundamenskii VS, Moskalev PN. *Sov. Phys. Crystallogr.* 1984; **29**: 273; de Cian A, Moussavi M, Fisher J, Weiss R. *Inorg. Chem.* 1985; **24**: 3165.
- [29] André JJ, Holczer K, Petit P, Riou MT, Clarisse C, Even R, Fourmigué M, Simon J. *Chem. Phys. Letters* 1985; **115**: 463.
- [30] Simon J, Toupance T. In *Comprehensive Supramolecular Chemistry*, Elsevier Science: Oxford, 1996; vol. 10, chap. 21.
- [31] Toupance T, Plichon V, Simon J, *New J. Chem.* 1999; **23**: 1001.

**TABLE:**

$r$	$M_w$ (g/mol)	$\beta$ ( $I \propto q^{-\beta}$ )
2	$1.1 \cdot 10^6$	2.3-2.6
8	$5.0 \cdot 10^6$	1.3
32	$1.0 \cdot 10^5$	1.0

**Table 1.** Molecular characteristics of the aggregates formed by [(15C5)<sub>4</sub>Pc]<sub>2</sub>Lu in presence of various amounts of KSCN in chloroformic based mixture solution ([**1**] = 10<sup>-5</sup> M in S98; KSCN 10<sup>-2</sup>M in S90).  $M_w$  is the weight-average molar mass.  $\beta$  is the scaling factor between the scattering intensity ( $I$ ) and the wave vector ( $q$ ).

## FIGURES CAPTIONS:

**Fig.1a.** Chemical formula of  $[(15C5)_4Pc]_2Lu$  (**1**) after reference [10] – Reproduced by permission of The Royal Society of Chemistry.

**Fig. 1b.** Schematic structure of the pillar-like aggregates of **1** formed in the presence of potassium ions after reference [12] – Reproduced by permission of the American Chemical Society.

**Fig. 2.** Chemical structure of the chemical derivative **2** used to graft an aminosilane functionalized silica surface. The molecule **2** is used as an anchoring site for the binding of pillar-like aggregates (selective binding site).

**Fig. 3.** Absorption spectra of **1** in S98 as a function of ratio  $r = [KSCN]/[1]$ . The figure shows the initial spectrum **a** ( $r = 0$ ), the final spectrum **b** ( $r = 5$ ) and the intermediate spectra corresponding to  $r = 0.5; 1; 1.5; 2; 2.5; 3; 3.5; 4; 4.5$ . Arrows indicate the spectroscopic changes. Inset: plot of the fraction of the monomer as a function of  $r$ .

**Fig. 4a.** AFM image of the aggregates of  $[(15C5)_4Pc]_2Lu/KSCN$  on silica  $SiO_2$  (immersing time: 10 min, concentration of **1**:  $10^{-5}$  M in S95, KSCN:  $1.6 \cdot 10^{-4}$  M). Image  $800 \times 800 \text{ nm}^2$ .

**Fig. 4b.** Profile section according to the line shown in Fig. 4a.

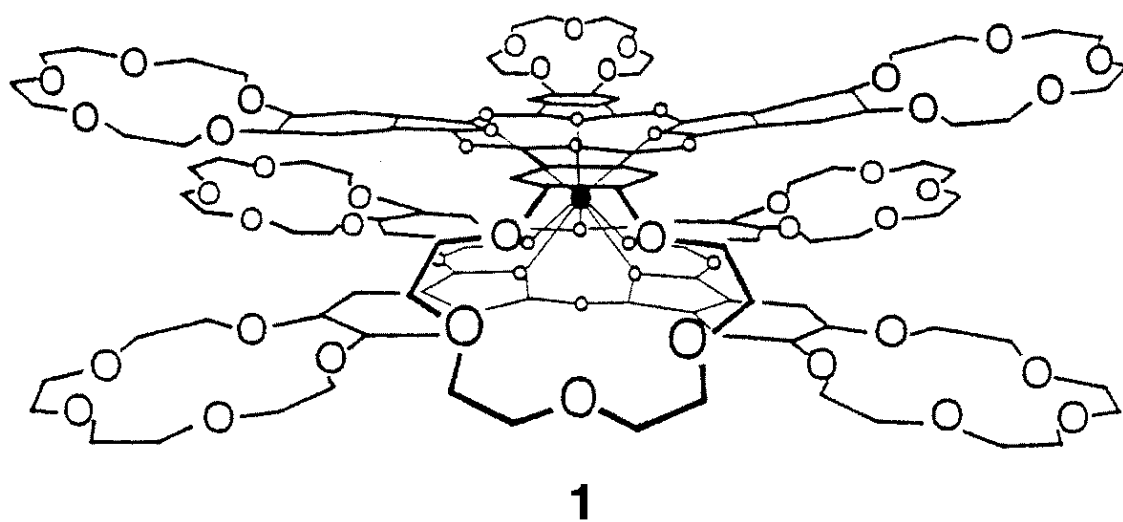
**Fig. 5a.** AFM image of the aggregates of [(15C5)<sub>4</sub>Pc]<sub>2</sub>Lu/KSCN on silica functionalized with 3-aminopropyl trimethoxysilane (immersing time: 3 min, concentration of **1**: 10<sup>-5</sup> M in S95, KSCN: 1.6 10<sup>-4</sup> M). Image 800×800 nm<sup>2</sup>.

**Fig. 5b.** Profile section according to the line shown in Fig. 5a.

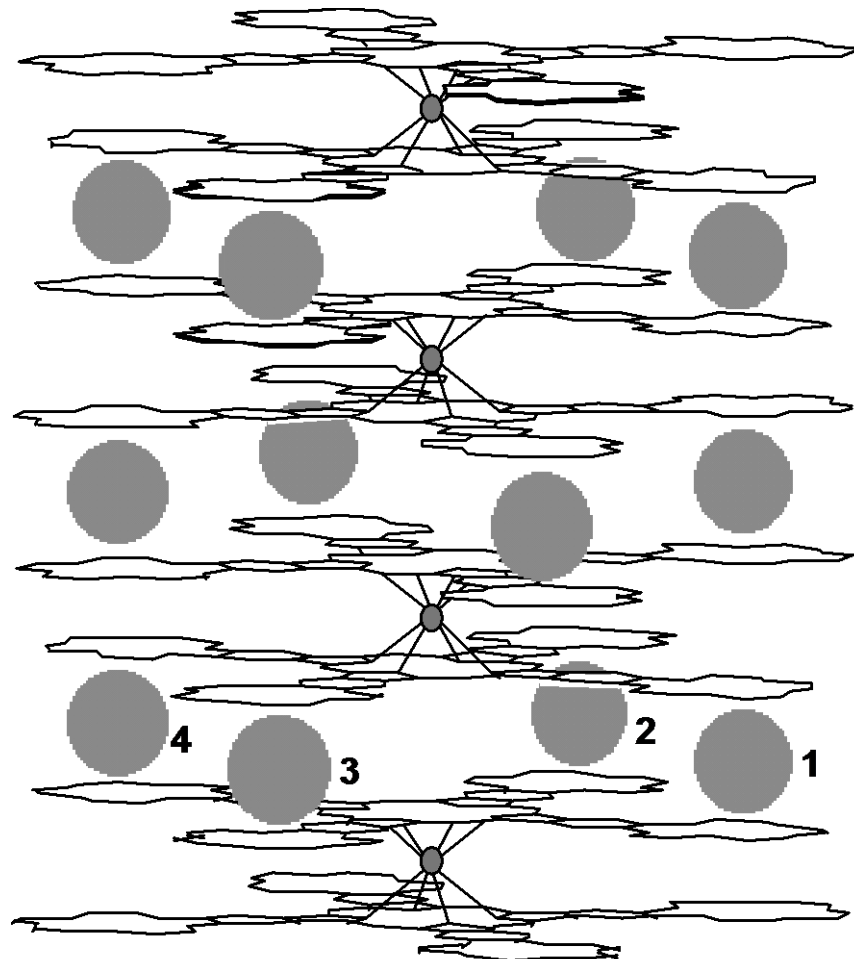
**Fig. 6a.** AFM image of the aggregates of [(15C5)<sub>4</sub>Pc]<sub>2</sub>Lu/KSCN on functionalized silica grafted with **2** (immersing time: 40 min, concentration of **1**: 10<sup>-5</sup> M, KSCN: 1.6 10<sup>-4</sup> M). Some aggregates are labelled from 1 to 8. Image 800×800 nm<sup>2</sup>. Note that the full scale of this image is equal to 30 nm and compare with Fig. 4a and 5a for which the aggregates are parallel to the surface (full scale 4 and 8 nm).

**Fig. 6b.** Profile section following the aggregates labelled in Fig 6a.

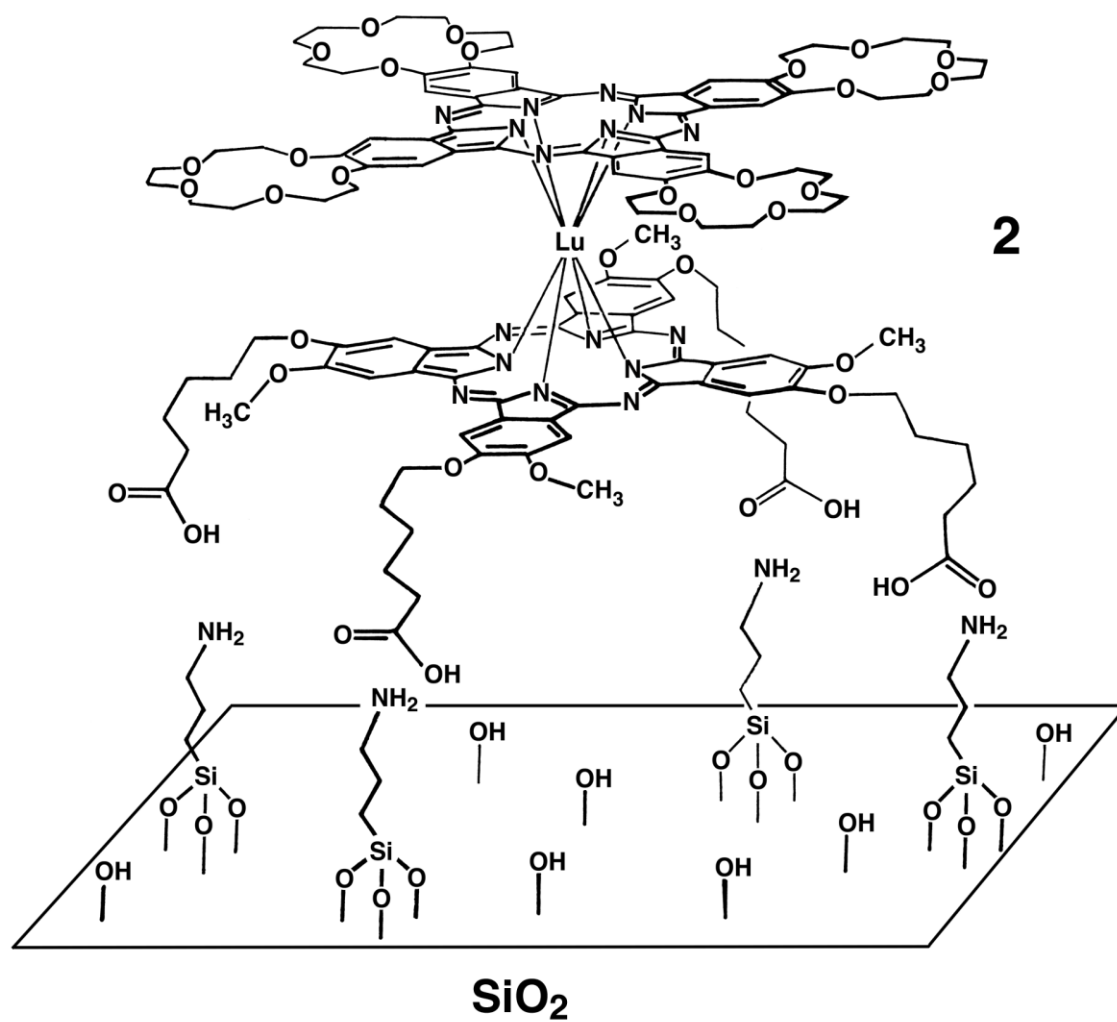
**Fig. 7.** AFM image showing the polygonal geometry of a single spot. This image has been obtained by using a sharp AFM tip (SuperSharpSilicon Nanosensors). Image 200×100 nm<sup>2</sup>.



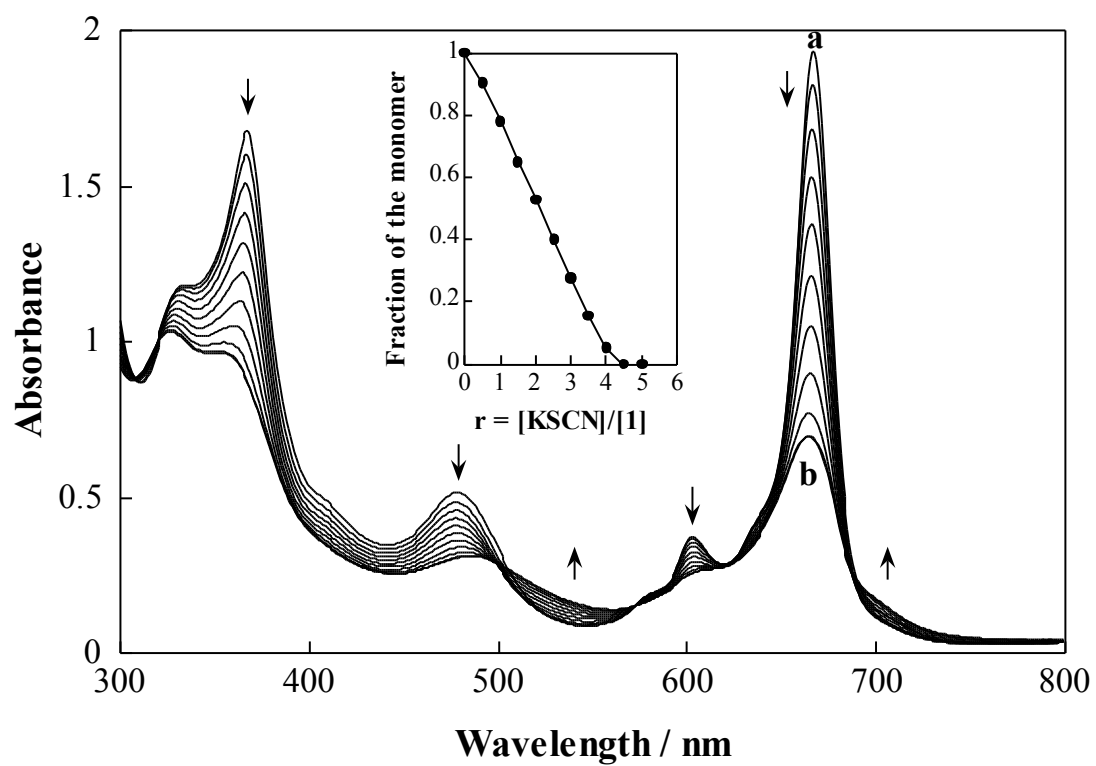
**Fig.1a**

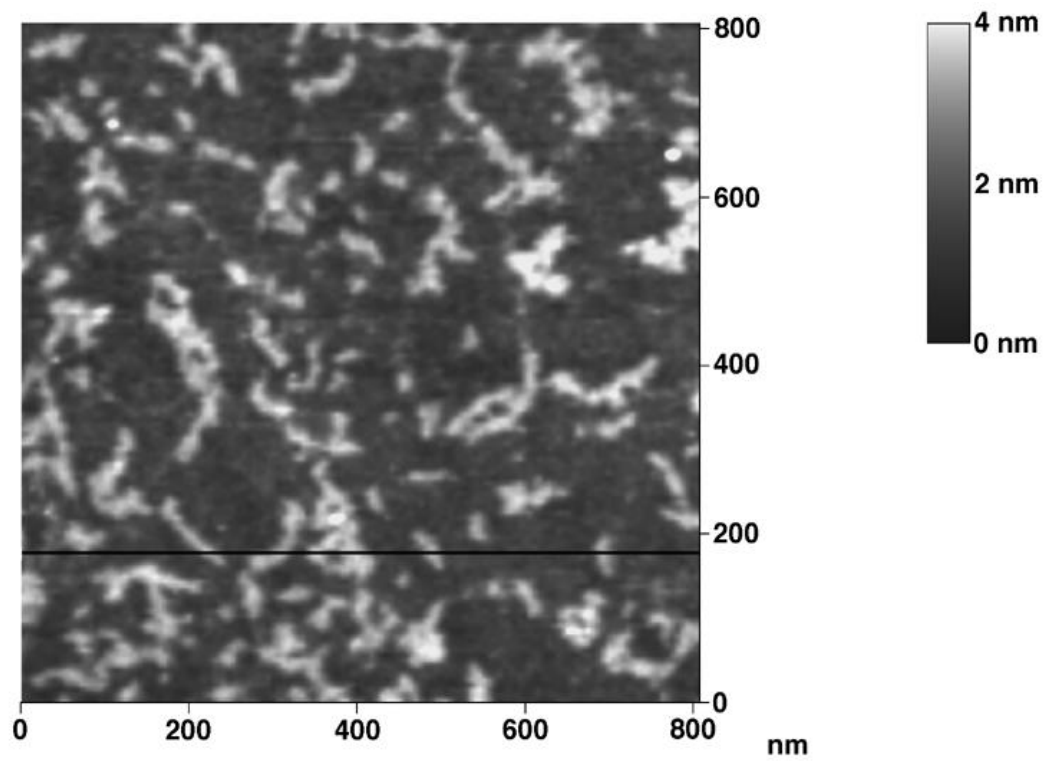
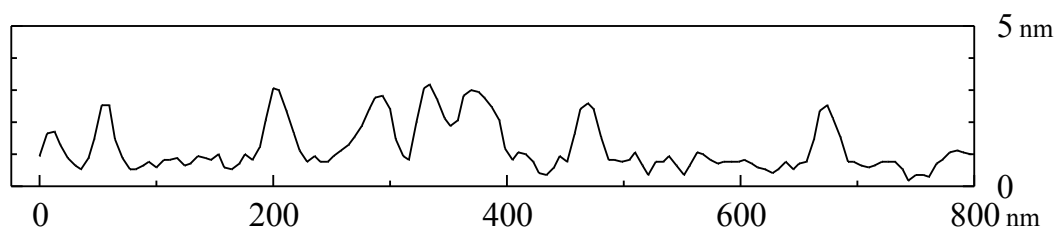


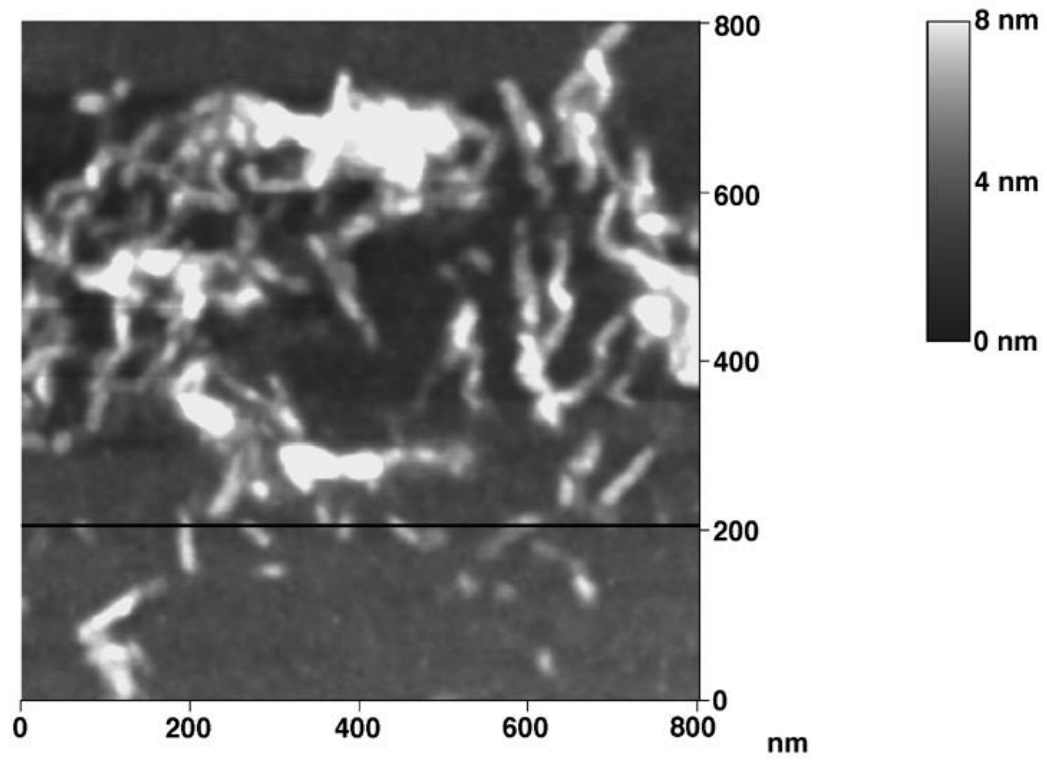
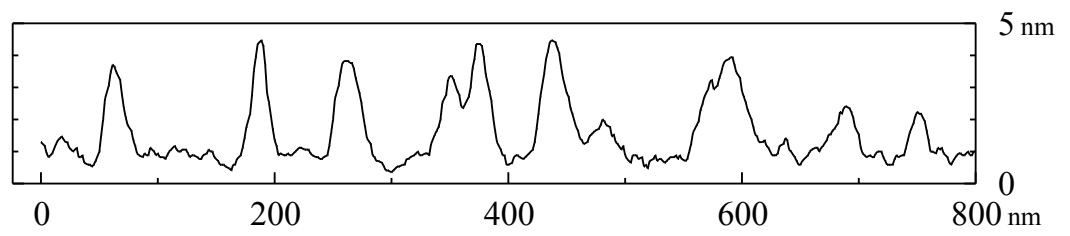
**Fig. 1b**

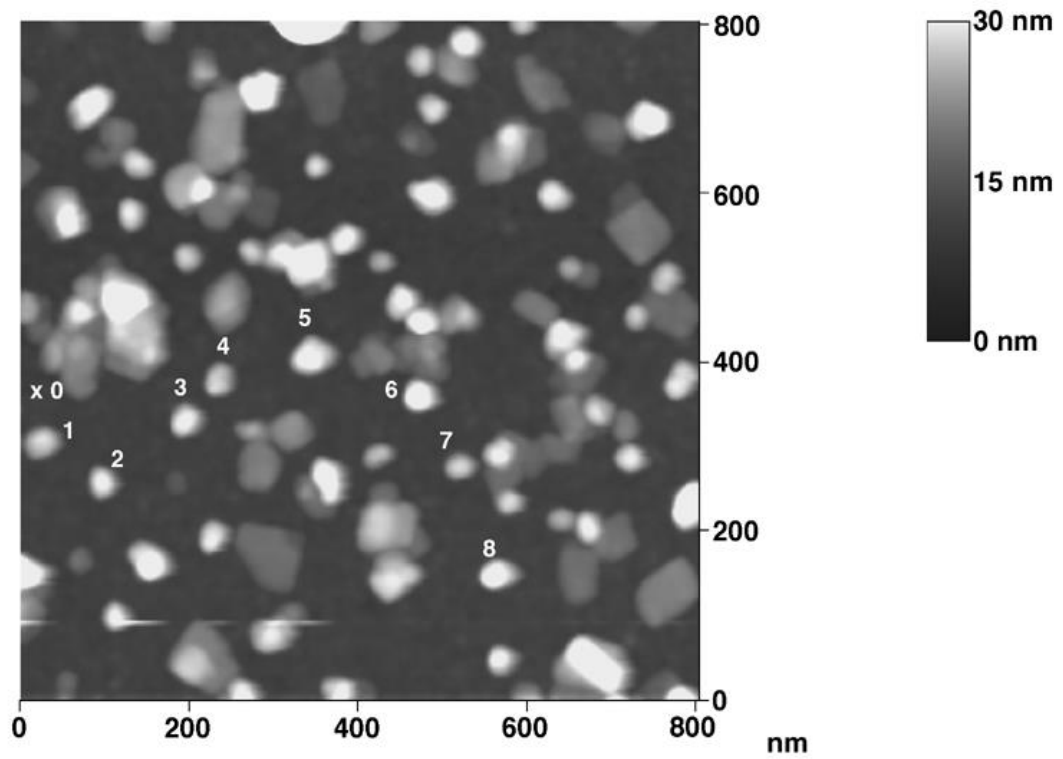
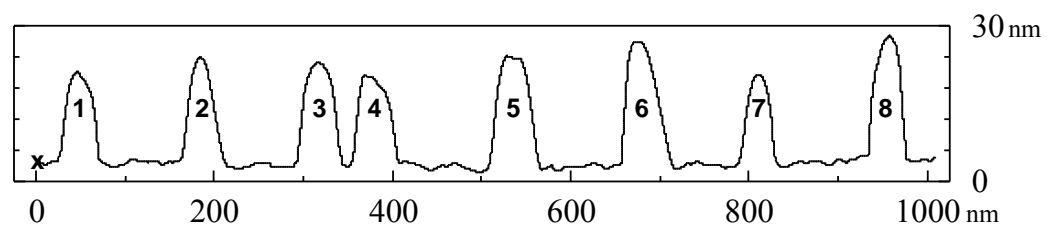
**Fig. 2**



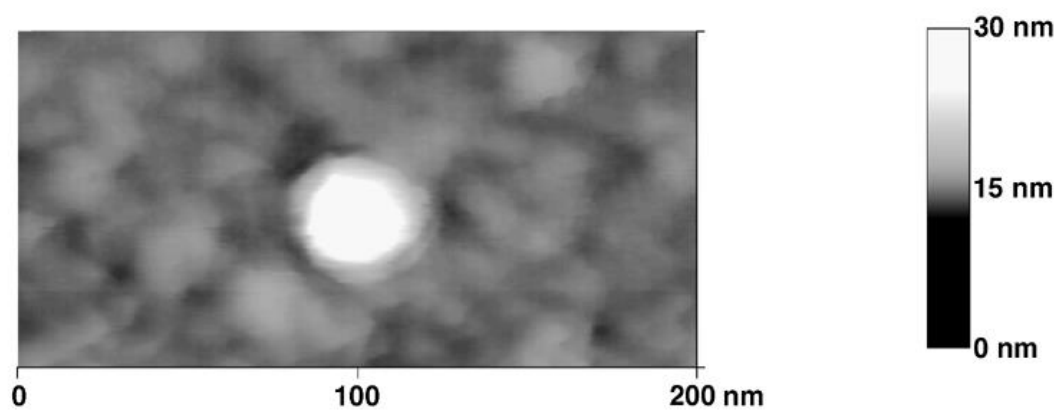
**Fig. 3**

**Fig. 4a****Fig. 4b**

**Fig. 5a****Fig. 5b**

**Fig. 6a****Fig. 6b**



**Fig. 7**